ACS OMEGA

http://pubs.acs.org/journal/acsodf

Article

Comparative Studies on Hydraulic Fracturing Fluids for High-Temperature and High-Salt Oil Reservoirs: Synthetic Polymer versus Guar Gum

Xiaoqin Cao, Yiwen Shi, Wenzhi Li, Peiyun Zeng, Zhuo Zheng, Yujun Feng, and Hongyao Yin*

Cite This: *ACS Omega* 2021, 6, 25421−25429

Read Online

ACCESS | Metrics & More | Article Recommendations

ABSTRACT: The increasing energy demand has prompted engineers to explore deeper wells where rich oil and gas reserves exist. However, the high-temperature and high-salt conditions have impeded the further application of traditional water-based fracturing fluids in such reservoirs. Therefore, it is urgent to develop fracturing fluids that are suitable for such geographic characteristics. In this study, for the first time, a novel synthetic polymer, poly-(acrylamide-*co*-acrylic acid-*co*-2-acrylamido-2-methyl-1-propanesulfonic acid) (P3A), was investigated as a rheological modifier for water-based fracturing fluids in high-temperature and high-salt conditions and compared with a guar gum system. Results showed that the apparent viscosity increased with increasing P3A and guar gum concentrations, and the thickening ability of P3A was much better than that of guar gum. Despite the better shear and temperature resistance and proppant suspension ability of guar gum fluids in high-temperature and saturated salt conditions, plentiful solid residues after gel-breaking have prevented their progress in the petroleum industry. P3A fluids have no residues, but the unsatisfying proppant suspension capability and high dosage encourage us to promote their rheological performance via interaction with an organic zirconium crosslinker. Infrared spectroscopy and scanning electron microscopy were applied to guarantee the successful reaction of P3A with the crosslinker. The subsequent investigation indicated that the transformed fracturing fluid exhibited remarkably improved thickening capability and satisfying rheological performance in terms of temperature and shear resistance and proppant-carrying ability as well as gel-breaking results in a high-temperature and saturated salt environment. All of the above results suggest the potential application of crosslinked P3A in hydraulic fracturing for the reservoirs with hostile conditions, and this article also provides a new orientation for synthetic polymers utilized in the oil and gas industry.

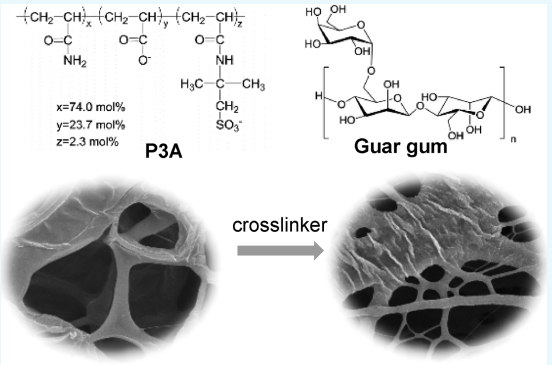

1. INTRODUCTION

Since its initial implementation in petroleum exploration, hydraulic fracturing has become the most mature and efficient technology and has been applied widely in the oil and gas industry to promote the productivity of hydrocarbon resources so as to solve the growing global energy crisis.[1,2] In the practical operation process, the pressurized fracturing fluid is injected into the wellbore to create fractures and transport proppants to keep the fractures open at the end of the hydraulic fracturing process, thus providing an effective pathway for the trapped hydrocarbon.[3,4] Over the past 70 years, water-based fracturing fluids have become increasingly popular in hydraulic fracturing owing to their eco-friendliness and safety compared to the oil-based ones.[5] To the best of our knowledge, water-soluble polymers are the most important ingredients to embellish the rheological performances of such fracturing fluids.[6] Rheological performances, including viscosity and shear and thermal resistance, are the key to ensuring the successful operation of hydraulic fracturing, and they are also the most vital point associated with researchers' concerns. In the past several decades, guar gum and its derivatives have become classic examples of biopolymers that are employed in fracturing fluids owing to their low cost, good environmental acceptance, and renewability as well as desired thickening ability.[5,7] Although they produce some residues, guar gum-based fracturing fluids still play an important role in the petroleum exploration industry.[8]

Synthetic water-soluble polymers are also applied in water-based fracturing fluids. Partially hydrolyzed polyacrylamide (HPAM) is considered as the vital representative of synthetic polymers and has been widely utilized in the petroleum

Received: June 29, 2021
Accepted: September 10, 2021
Published: September 21, 2021

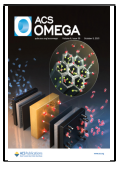

https://doi.org/10.1021/acsomega.1c03394
ACS Omega 2021, 6, 25421−25429

extraction industry owing to its low cost and high efficiency.[9−11] In HPAM solution, the strong intra- and interchain electrostatic repulsions of the carboxylate group lead to remarkable thickening ability in freshwater and at a relatively low temperature (<75 °C).[12,13] However, previous studies have shown that HPAM is highly sensitive in electrolyte solution as the charge shielding effect of inorganic cations to carboxylate groups makes the polymer chain collapse, which leads to a macroscopic viscosity decline.[14−16] Thus, great efforts have been made to conquer the salt intolerance of HPAM. Copolymerization of acrylamide (AM) with functional monomers such as 2-acrylamide-2-methyl propanesulfonic acid (AMPS), vinylpyrrolidone, and *N*-(1,1-dimethyl-3-oxobutyl)-acrylamide is an alternative strategy to enhance salt insensitivity.[17−20] For example, our group recently reported on a thermoviscosifying polymer composed of AM and *N*-(1,1-dimethyl-3-oxobutyl)-acrylamide.[19] Results indicated that such thermoviscosifying polymer-based fracturing fluid exhibited a satisfying thickening performance in a high-salt environment. However, the functional monomer is expensive, and such a polymer is so complex to synthesize that it is limited of large-scale development in practical applications.

It is predicted that the rising population will drive up the energy demand from 85 million barrels per day at present to 106 million barrels per day by 2030.[21] One way to meet such a huge demand is to exploit oilfields sufficiently. Traditional low- to medium-salt and mild-temperature oilfields have been developed exhaustedly, which have made it difficult to solve the coming energy crisis.[22] Thus, more attention has been given to deeper reservoirs where rich crude oil and gas reserves exist.[23] For example, the Jianghan Oilfield in China contains abundant shale gas resources about 9.1×10^{12} m^3,[24] and the original oil in place of Tarim Oilfield in China is up to about 300 million tons.[23] However, such deep wells are often associated with the high-salt environment, which prevents a mass of polymers as a rheological modifier for fracturing fluids to apply in these formations. For instance, the salt is over 26×10^4 mg·L^{-1} in Jianghan Oilfield and over 11×10^4 mg·L^{-1} in Tarim Oilfield. Moreover, some reservoirs are accompanied by high temperatures, *e.g.*, Tarim Oilfield, which are always over 100 °C. To make the most of deep reservoirs, novel polymers should be exploited to promote the rapid expansion of fracturing fluids in such harsh geological conditions.

Recent research from our group suggested that polyelectrolyte complexes containing modified HPAM, poly-(acrylamide-*co*-acrylic acid-*co*-2-acrylamido-2-methyl-1-propanesulfonic acid) (P3A), and poly[2-(methacryloyloxy)-ethyl] trimethyl ammonium chloride (PDMC) show good rheological properties in high-temperature and high-salt conditions.[25] However, expensive PDMC and a high polymer concentration impede the large-scale application of such polyelectrolyte complexes in practical manipulation. Owing to the existence of a salt-tolerance monomer (AMPS) in the molecular backbone of P3A, the excellent salt resistance of such a polymer promises applicability in saliferous environments. However, the systemic study of P3A as a rheological modifier for fracturing fluids in high-temperature and high-salt conditions has not been conducted yet. Therefore, in this study, for the first time, the rheological performances of P3A solutions were investigated in high-temperature and high-salt conditions and compared with guar gum solutions, whose rheological properties are also absent in the same conditions. Scheme 1 shows the molecular structure of P3A and guar gum.[25,26] Results suggested that both P3A and guar gum

Scheme 1. Molecular Structures of P3A and Guar Gum

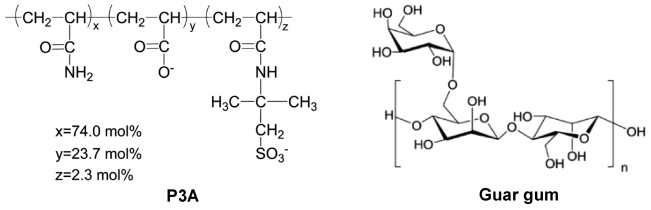

systems exhibit good rheological performance. Nevertheless, many residues of guar gum solutions after gel breaking have impeded the further application. Despite there being no residues, the poor proppant suspension ability and high dosage of P3A solutions encouraged us to improve their microscopic structure via interaction with organic zirconium (abbreviated to Zr). The evolved P3A was investigated as a rheological modifier for fracturing fluids, and the corresponding results indicated that the crosslinked P3A system revealed satisfying rheological properties even at a 0.6 wt % polymer concentration.

2. RESULTS AND DISCUSSION

2.1. Dissolution Property. The dissolvability of a polymer in solvent is the first step to obtaining an excellent viscous fluid. Figure 1A,B displays the photographs of 1.0 wt % P3A

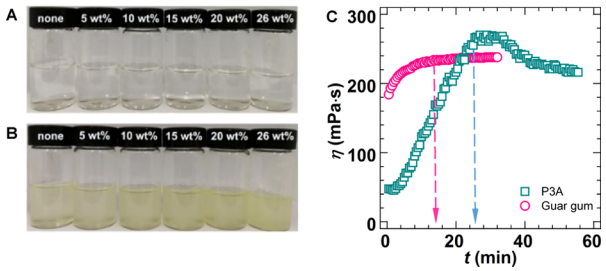

Figure 1. Snapshots of (A) 1.0 wt % P3A and (B) 1.0 wt % guar gum in different solutions with NaCl concentrations ranging from 0 to 5.0, 10.0, 15.0, 20.0, and 26.0 wt %. (C) Determination of dissolution time of 1.0 wt % P3A and guar gum in saturated brine.

and guar gum dissolved in aqueous solution with different NaCl concentrations ranging from 0 to 5.0, 10.0, 15.0, 20.0, and 26.0 wt %. The concentration of saturated NaCl solution is 26.0 wt %. Both the P3A and guar gum solutions were transparent and had no sediment, indicating that 1.0 wt % samples can completely dissolve in various NaCl aqueous solutions. Notably, the solutions in Figure 1B are light yellow in color, which is attributed to the inherent nature of guar gum. To explore the dissolution velocity, the dissolution times of 1.0 wt % P3A and guar gum in saturated NaCl solution were tested, as shown in Figure 1C. The apparent viscosity of guar gum and P3A rose quickly and remained stable after 14 and 26 min, respectively, implying their fast dissolution speed. In comparison with guar gum, P3A showed a relative longer dissolution time, presumably owing to its high molecular weight, which needs more swelling time.

2.2. Rheological Properties. *2.2.1. Thickening Ability.* The performance of fracturing fluids is greatly controlled via

https://doi.org/10.1021/acsomega.1c03394
ACS Omega 2021, 6, 25421−25429

the thickening ability of polymers; thus, the dominating factors of polymer thickening ability should be inspected. Figure 2A,C

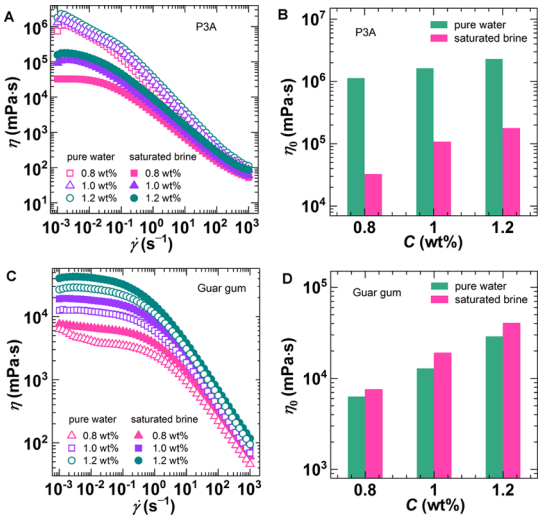

Figure 2. (A) Steady-state flow curves of P3A with concentrations of 0.8, 1.0, and 1.2 wt %. (B) η_0 as a function of P3A concentration in pure water and saturated brine. (C) Steady-state flow curves of guar gum with concentrations of 0.8, 1.0, and 1.2 wt %. (D) η_0 as a function of guar gum concentration in pure water and saturated brine (25 °C; shear rate, 0.001−1000 s^{-1}).

depicts the steady-state flow curves of P3A and guar gum with concentrations ranging from 0.8 to 1.0 and 1.2 wt % in pure water and saturated brine. It was obvious that the apparent viscosity of all of the samples declined with the increase in shear rate and augmented with increasing polymer concentration. The remarkable shear-thinning phenomenon is the representative symbol of non-Newtonian fluid. Additionally, at a low shear rate, a constant viscosity was observed. The plateau value at a low shear rate was regarded as zero-shear viscosity (η_0), which is the significant estimate factor of the rheological property. The higher the η_0 is, the stronger the interaction of polymer molecular chain becomes, and the stronger network results in better rheological performance. However, in Figure 2A, in the pure water system, the constant viscosity disappeared and was replaced by instant viscosity (the vertex of the curve), which was also considered as η_0. Figure 2B,D represents the relational graph of concentration and η_0 of P3A and guar gum in pure water and saturated brine, respectively. It was distinct that the η_0 values rose with the polymer concentration augmented in either pure water or saturated NaCl solution. Interestingly, for the P3A solutions in the same concentration, the η_0 values in saturated brine were much less than that in pure water, which indicates that NaCl may affect the thickening ability of P3A. The η_0 values in saturated brine were 3.27 × 10^4, 10.8 × 10^4, and 17.8 × 10^4 mPa·s for P3A, while the corresponding values in pure water were 113 × 10^4, 163 × 10^4, and 229 × 10^4 mPa·s, respectively. For the guar gum solutions, an interesting phenomenon was observed that at the same polymer concentration, the η_0 values in pure water were lower instead of higher than that in saturated brine, which was inconsistent with the behavior of P3A solutions (Figure 2D). The inconsistent phenomenon is described as below. For P3A in saturated brine, the inorganic ions can cause the polymer chains to be coiled by the charge shielding effect, thus lowering the thickening efficiency. For guar gum in saturated brine, the screening effect of inorganic ions is limited because it has no negative charge on the molecular chains. The slightly increasing viscosity of guar gum in saliferous solution might be owing to the transformation of disorder polymer molecular chains to a regular helix structure in the effect of inorganic ions, resulting in stronger networks. The η_0 values of guar gum in saturated brine were 7.57 × 10^3, 1.91 × 10^4, and 4.04 × 10^4 mPa·s, while the corresponding values in pure water were 6.31 × 10^3, 1.29 × 10^4, and 2.9 × 10^4 mPa·s, respectively. When we compared Figure 2B and Figure 2D, an interesting phenomenon was observed that the η_0 values of P3A solutions were much higher than those of guar gum solutions in the same circumstances. The corresponding differences were about 4, 5, and 4 times in saturated brine and 179, 126, and 79 times in pure water, respectively. These great differences indicate that despite being influenced by NaCl, the thickening ability of P3A is still better than that of guar gum in either saturated brine or pure water.

Further investigation of NaCl affection for the viscosity behavior of polymer solution is indispensable as fracturing fluids are mainly applied in a saliferous environment. Figure 3A,B displays the steady-state flow curves of 1.0 wt % P3A and guar gum in various NaCl concentrations from 0 to 5.0, 10.0, 15.0, 20.0, and 26.0 wt %. The shear thinning behavior of all of the specimens was evident with increasing shear rate, and constant values emerged in a low shear rate of all of the curves. The corresponding plots of η_0 with various NaCl concentrations of P3A and guar gum solutions are presented in Figure 3C. For the P3A system (green square), the η_0 value in pure water declined sharply when 5 wt % NaCl existed, a reduction of 88.6% from 163 × 10^4 to 18.6× 10^4 mPa·s. Further increasing the NaCl species from 10.0 to 15.0, 20.0 and 26.0 wt % in P3A solution, the η_0 values declined slowly from 11.4 × 10^4 to 10.7 × 10^4, 9.11 × 10^4, and 10.8 × 10^4 mPa·s, respectively. The decimated η_0 values in saliferous solution suggest that P3A is highly sensitive for salt solution. However, for the guar gum system (red circle), an increase rather than

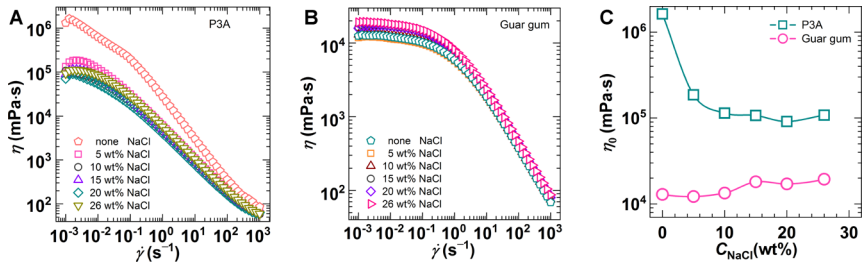

Figure 3. Steady-state flow curves of (A) 1.0 wt % P3A and (B) 1.0 wt % guar gum in 0, 5.0, 10.0, 15.0, 20.0, and 26.0 wt % NaCl contents. (C) η_0 as a function of NaCl concentration (25 °C; shear rate, 0.001−1000 s^{-1}).

https://doi.org/10.1021/acsomega.1c03394
ACS Omega 2021, 6, 25421−25429

decrease was occurred for the η_0 values; that is, it slightly rose from 1.29×10^4 to 1.22×10^4, 1.34×10^4, 1.81×10^4, 1.71×10^4, and 1.91×10^4 mPa·s in the corresponding NaCl solution, respectively, indicating the negligible effect of NaCl. Analysis results suggest that P3A is more sensitive than guar gum for NaCl solution.

2.2.2. Temperature and Shear Resistance. Thermal and shear resistance should be considered as fracturing fluids are often subjected to strong mechanical shear and temperature in the hydraulic fracturing process. Figure 4A,B shows the

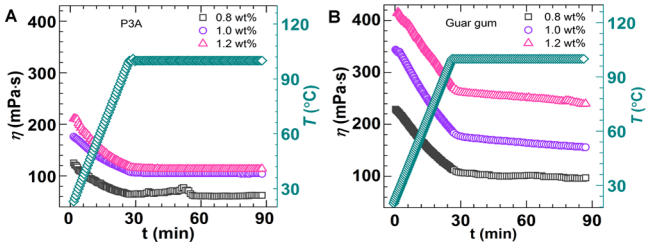

Figure 4. Apparent viscosity as a function of shear time for (A) P3A and (B) guar gum solutions with various concentrations in saturated brine at 20−100 °C (shear rate, 170 s^{-1}).

rheological curves of P3A and guar gum in saturated brine at a temperature scanning from 20 to 100 °C with a shear rate of 170 s^{-1} (according to the oil and gas industry standard of the People's Republic of China (SY/T 6367−2008)), respectively. A distinct phenomenon was discovered: The apparent viscosity of all of the sample solutions decreased sharply when the temperature increased, while a relatively stable viscosity was observed at a constant temperature. The thermal thinning behavior of all of the samples was characterized by thermal dilation as most water-soluble polymer solutions are. Nevertheless, the guar gum solutions still maintained a higher apparent viscosity than P3A solutions in the same concentration, and the final values reached 97, 156, and 240 mPa·s for the guar gum system, as compared with 63, 104, and 114 mPa·s for the P3A system, respectively. All of the final viscosity values met the industrial standard (>50 mPa·s), and the temperature and shear resistance of guar gum systems was better than that of P3A systems.

2.3. Proppant-Carrying Ability. One of the main functions of fracturing fluid is to transport proppants along the length of fractures and to maintain them in suspension throughout the hydrofracking operation process. Figure 5A,B shows the photographs of silica sand suspension time in P3A and guar gum solutions at the concentrations of 0.8, 1.0, and 1.2 wt % in saturated brine at 100 °C, respectively. It is obvious that the suspension time augmented with increasing polymer concentration in both P3A and guar gum systems, suggesting that viscosity is a factor that affects the transport proppant property of fracturing fluids. The final suspension times were 0.5, 1.0, and 2.0 h of different P3A solutions, compared with 1.0, 1.5, and 2.0 h of different guar gum solutions, respectively. The above results indicate that the proppant suspension ability of P3A systems is slight weaker than that of guar gum systems.

2.4. Gel-Breaking Results. The excess residues and long-time stay of fracturing fluids in the wellbore will lead to irretrievable reservoir damage. According to the oil and gas industry standard of the People's Republic of China (SY/T 6367−2008), the fracturing fluid must be broken in the allowable time with no or a few residues. The requirement for

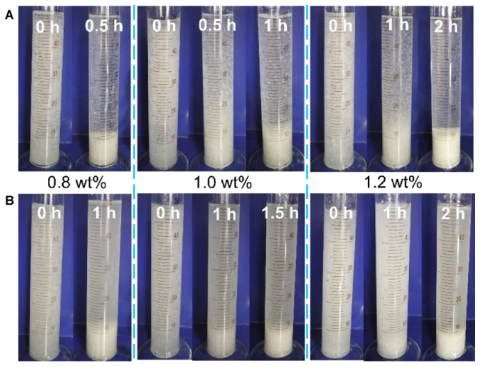

Figure 5. Representative photographs of different time periods of proppants mixed with either (A) P3A or (B) guar gum with various concentrations in saturated brine at 100 °C (20−50 mesh).

gel-breaking time (t_b) is less than 720 min when the viscosity (η_f) is smaller than 5 mPa·s, and the residues should be less than 6×10^2 mg/L. Table 1 lists the gel-breaking results of

Table 1. Gel-Breaking Results of P3A and Guar Gum Solutions at 100 °C

	0.1 wt % APS			0.2 wt % APS		
$C_{polymer}$ (wt %)	η_f (mPa·s)	residues (mg/L)	t_b (min)	η_f (mPa·s)	residues (mg/L)	t_b (min)
			P3A			
0.8	2.34	none	90	2.43	none	60
1.0	2.37	none	90	3.82	none	60
1.2	2.71	none	90	2.83	none	60
0.8[a]	2.43	none	90			
			guar gum			
0.8	1.82	1020	100	1.68	813	100
1.0	2.56	1170	100	2.24	865	100
1.2	1.97	1540	100	1.81	928	100
0.8[a]	4.78	480	100			

[a]In a pure water system.

P3A and guar gum systems with concentrations of 0.8, 1.0, and 1.2 wt % after using different amounts of APS as the gel breaker at 100 °C. As Table 1 shows, for P3A systems at the same concentration, the gel-breaking times became shorter at higher APS dosages. At 0.1 and 0.2 wt % APS concentrations, the gel-breaking times of all of the P3A samples were 90 and 60 min, respectively. Importantly, there were no residues of any of the tested samples even with the saturated NaCl solution. Compared with guar gum systems, when the same APS dosage was employed in the saturated brine, the residues increased with the addition of guar gum concentration. The residues of different guar gum concentrations were 1.02×10^3, 1.17×10^3, and 1.54×10^3 mg/L in 0.1 wt % APS and were 8.13×10^2, 8.65×10^2, and 9.28×10^2 mg/L in 0.2 wt % APS, respectively, which are higher than the industrial standard.

To investigate the affection of salt for the gel-breaking results, 0.8 wt % P3A and guar gum in pure water were used for experimentation, and the results are reported in Table 1. None of the residues of the P3A system could be found, while just a few of the residues existed in the guar gum solution (4.8×10^2 mg/L). The results suggest that the gel-breaking residues of guar gum are influenced by salt greatly. According to the table date, the gel-breaking time of P3A solutions was less than that of the guar gum solutions, while the residues of guar gum

https://doi.org/10.1021/acsomega.1c03394
ACS Omega 2021, 6, 25421−25429

systems were much higher than those of the P3A systems, indicating that guar gum can potentially damage reservoirs.

In summary, although the guar gum solutions displayed good viscosity and temperature and shear resistance, many residues in a high-temperature and high-salt environment limit the further use of such species in the oil recovery process. Synthetic polymer P3A solutions can be employed in the hydraulic fracturing process based on the negligible reservoir-damage potential, but the high dosage and unsatisfying proppant suspension ability prevent its practical usability. Previous studies suggested that the reaction of polymer function groups with a crosslinker results in the strengthening of the network structure, which can promote the viscosity of the polymer solution greatly and reduce dosage.[11,27] Thus, we further investigated the rheological properties of crosslinked P3A fluid in saturated NaCl conditions.

2.5. Crosslinked P3A Hydrofracking Fluid. *2.5.1. Crosslinking Mechanism.* Figure 6A,B displays the representative

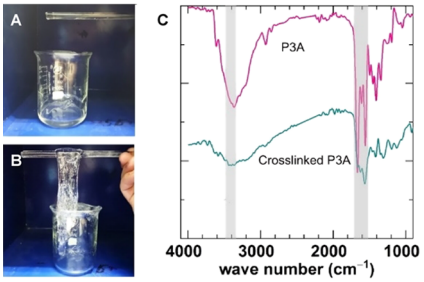

Figure 6. Representative photographs of 0.8 wt % P3A brine solution (A) without and (B) with a Zr crosslinker. (C) IR spectra of P3A with and without a Zr crosslinker.

photographs of P3A fluid with and without a Zr crosslinker. It was clear that the original P3A solution was hardly picked up by a glass rod, while the crosslinked one was easily picked up. Then, the IR spectrum was employed to investigate the crosslinking mechanism, and the corresponding spectra of P3A (red curve) and crosslinked P3A (green curve) are shown in Figure 6C. The absorption band at 3369 cm^{-1} was ascribed to the stretching vibration of N−H in AM, and the bands at 2925 and 2851 cm^{-1} corresponded to the asymmetrical and symmetrical stretching vibrations of $-CH_2-$ in the backbone, respectively. In addition, the absorption peaks at 1644 and 1610 cm^{-1} occurred because of the stretching vibration of C═O and the flexural vibration of N−H in AM, respectively. Further, the peak at 1566 cm^{-1} was attributed to the asymmetrical stretching vibration of the carboxylate anion of AA, and the peak at 1411 cm^{-1} was imputed to the mixed in-plane flexural vibration of C−N and N−H of AM. Apart from that, the absorption bands at 1191, 1105, and 1057 cm^{-1} were attributed to the asymmetrical and symmetrical stretching vibrations of the S═O group in AMPS, respectively.[11,28] The IR spectrum of the crosslinked copolymer was also displayed (green curve). The absorption bands at 3416, 2934, and 2890 cm^{-1} were imputed to the stretching vibration of N−H in AM and asymmetrical and symmetrical stretching vibrations of $-CH_2-$ in the polymer backbone, respectively. Similarly, the peaks at 1658, 1619, and 1572 cm^{-1} were ascribed to C═O and N−H in AM and the carboxylate anion in AA, respectively. The absorption band at 1414 cm^{-1} occurred due to the mixed in-plane flexural vibration of C−N and N−H of AM, and the absorption bands at 1203, 1120, and 1059 cm^{-1} came down to the asymmetrical and symmetrical stretching vibrations of the S═O group in AMPS, respectively.[29] From these analyses, we observed that after mixing with Zr, the main absorption bands of P3A exhibited a slight redshift, suggesting the successful interaction of the P3A functional group with Zr species.

Figure 7A,C demonstrates the low-magnification SEM images of 0.1 wt % P3A fluid without and with Zr species,

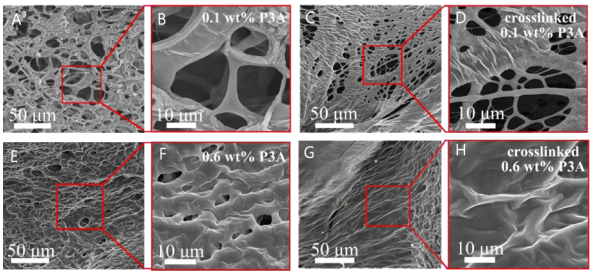

Figure 7. (A) Low-magnification and (B) high-magnification SEM images of 0.1 wt % P3A. (C) Low-magnification and (D) high-magnification SEM images of 0.1 wt % crosslinked P3A. (E) Low-magnification and (F) high-magnification SEM images of 0.6 wt % P3A. (G) Low-magnification and (H) high-magnification SEM images of 0.6 wt % crosslinked P3A.

respectively. It is clear that both of the pictures exhibit a complex porous network structure. The high-magnification SEM images further reveal that after crosslinking with Zr, a more complex network structure formed in the pore structure (Figure 7D), while the original sample just shows a sparse porous structure (Figure 7B). When increasing the polymer concentration to 0.6 wt %, a porous structure can be seen in Figure 7E,F of the original P3A, and a denser structure is shown in Figure 7G,H after Zr was inducted. Based on the previous report, the crosslink mechanism ascribed to the ligand exchange of some of the original zirconium ligands are replaced by the carboxylate group.[28] The three-dimensional structure of Zr is exhibited in Scheme 2A according to the literature,[30,31]

Scheme 2. (A) Three-Dimensional Structure of a Zr Crosslinker; (B) Crosslink Reaction of P3A with Zr

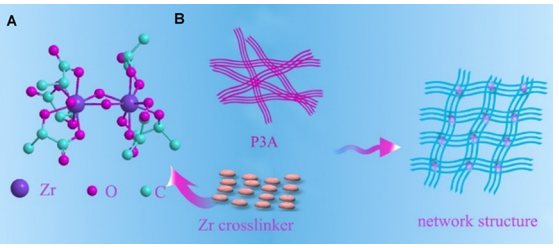

and the crosslinked progress is demonstrated in Scheme 2B. When the reaction took place, the carboxylate group in the polymer progressively replaced the lactate group in Zr. As the reaction is highly exothermic, which favors the exchange of lactate ligands for acrylate ones.[32−34] In conclusion, all of the results indicate the successful preparation of crosslinked P3A.

2.5.2. Thickening Ability. The concentrations of P3A and Zr are the dominating factors that affect the viscosity of crosslinked polymer solutions, and such an influence on polymer thickening ability was investigated. Figure 8A shows the steady-state rheological curves of 0.8 wt % P3A solution uncrosslinked and crosslinked with Zr. It was obvious that the

https://doi.org/10.1021/acsomega.1c03394
ACS Omega 2021, 6, 25421−25429

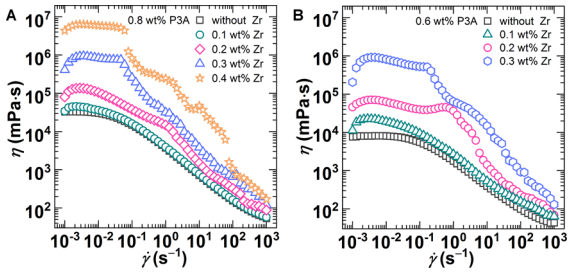

Figure 8. (A) Steady-state flow curves of (A) 0.8 wt % and (B) 0.6 wt % P3A solutions with various concentrations of Zr in saturated brine at 25 °C (shear rate, 0.001−1000 s^{-1}).

apparent viscosity of all samples reduced with increasing shear rate. When 0.1 wt % Zr was introduced, the η_0 value was just slightly higher than that of the uncrosslinked sample (4.54×10^4 mPa·s vs 3.27×10^4 mPa·s), and an overt increase in η_0 values occurred with further addition of Zr. In fact, when 0.4 wt % Zr existed, the crosslinked solution was so glutinous that it would be inappropriate to implement in practice. Thus, 0.2 or 0.3 wt % Zr is the suitable concentrations to use in further experiments. To reduce costs and protect the environment, further reduction of the dosage of the polymer is necessary. Figure 8B exhibits the rheological curves of the 0.6 wt % polymer solution interaction with or without Zr. There was no doubt that all of the samples displayed non-Newtonian fluid properties, and the η_0 values increased with increasing Zr content. The corresponding values of P3A solutions with 0.1, 0.2, and 0.3 wt % Zr contents were 2.26×10^4, 7.11×10^4, and 92.1×10^4 mPa·s for 0.6 wt %, compared with 4.54×10^4, 13.7×10^4, and 93.6×10^4 mPa·s for 0.8 wt %, respectively. In short, all of the results suggest that the crosslink reaction can greatly improve the viscosity of polymer solutions even in a lower polymer concentration.

2.5.3. Temperature and Shear Resistance. The strong mechanical shear and high temperature in oilfields may weaken the viscosity and sand suspension ability of fracturing fluids when injected into the wellbore. Thus, it is important to evaluate the shear and temperature resistance of the objective fracturing fluid. Figure 9A,B shows the rheological curves of

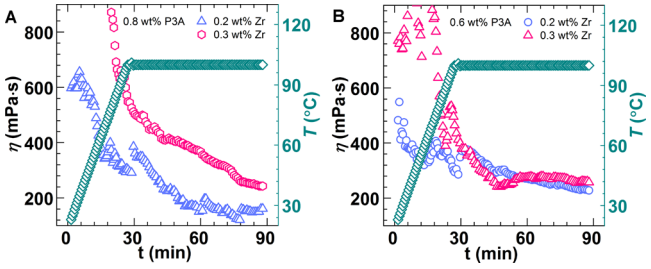

Figure 9. Apparent viscosity as a function of shear time of (A) 0.8 wt % P3A and (B) 0.6 wt % P3A crosslinked with various Zr concentrations in saturated brine at temperatures of 20−100 °C (shear rate, 170 s^{-1}).

temperature scanning of 0.8 and 0.6 wt % P3A solutions crosslinked with 0.2 and 0.3 wt % Zr in saturated NaCl solutions, respectively. The apparent viscosity of all of the sample solutions decreased sharply with increasing temperature and reduced slowly with constant temperature upon the increase in time. The final viscosity values of these specimens were 195 and 220 mPa·s of 0.8 wt % P3A solutions and were 200 and 224 mPa·s of 0.6 wt % P3A solutions with 0.2 and 0.3 wt % Zr, respectively, which were far superior values to the industrial standard (>50 mPa·s). The final viscosity values are a vital parameter to reflect the temperature and shear tolerance of polymer solutions. Therefore, we compared the final viscosity values of P3A, guar gum, and crosslinked P3A directly, and the corresponding results are shown in Table 2.

Table 2. Final Viscosity Values (η_f) of P3A, Guar Gum, and Crosslinked P3A Fluids at the Temperature and Shear Resistance Test

	P3A			guar gum		
C_P (wt %)	0.8	1.0	1.2	0.8	1.0	1.2
η_f (mPa·s)	63	104	114	97	156	240
	crosslinked P3A					
C_P (wt %)	0.8			0.6		
C_{Zr} (wt %)	0.2	0.3		0.2	0.3	
η_f (mPa·s)	195	220		200	224	

2.5.4. Proppant-Carrying Ability. In the laboratory proppant-carrying experiment, four types of crosslinked samples (0.8 wt % P3A + 0.2 wt % Zr, 0.8 wt % P3A + 0.3 wt % Zr, 0.6 wt % P3A + 0.2 wt % Zr, and 0.6 wt % P3A + 0.3 wt % Zr) were investigated in saturated NaCl solution at 100 °C, and the corresponding results are shown in Figure 10.

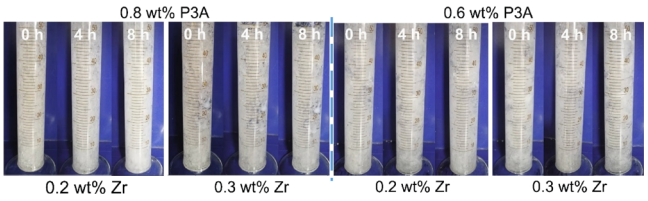

Figure 10. Representative photographs of different time periods of proppants mixed with either 0.8 wt % or 0.6 wt % P3A solutions crosslinked with different Zr concentrations in saturated NaCl solution at 100 °C (20−50 mesh).

Beyond our expectation, the proppants exhibited almost no submergence in either a 0.8 wt % or 0.6 wt % crosslinked P3A system after 8 h. The unrivalled proppant-carrying ability was ascribed to both the dense 3D network structures, which tightly held the proppants, and the strong crosslink bond, which survived in a high-temperature and high-salt environment.

2.5.5. Gel-Breaking Results. Table 3 lists the gel-breaking results of different crosslinked P3A solutions by using different amounts of APS at 100 °C. As the table shows, the t_b values

Table 3. Gel-Breaking Results of Crosslinked P3A Fluids at 100 °C

	0.1 wt % APS			0.2 wt % APS		
C_{Zr} (wt %)	η_f (mPa·s)	residues (mg/L)	t_b (min)	η_f (mPa·s)	residues (mg/L)	t_b (min)
0.8 wt % P3A						
0.2	2.17	283	90	3.22	140	60
0.3	3.23	158	90	3.18	120	60
0.6 wt % P3A						
0.2	4.31	55	120	3.44	60	90
0.3	4.96	175	120	4.12	202	90

https://doi.org/10.1021/acsomega.1c03394
ACS Omega 2021, 6, 25421−25429

decreased with increasing APS dosage for the same crosslinked P3A fracturing fluid system and increased with declining P3A concentration at the same APS dosage. The gel-breaking times of all of the crosslinked 0.8 and 0.6 wt % P3A solutions were 90 and 120 min of 0.1 wt % APS and were 60 and 90 min of 0.2 wt % APS, respectively. It was found that residues were still present in the broken fluids but much less than 6×10^2 mg/L. Even so, all of the gel-breaking results suggest that the crosslinked P3A fluid satisfies the needs of the professional standard.

3. CONCLUSIONS AND PERSPECTIVE

In conclusion, the rheological features of a synthetic salt-resistant polymer P3A and the biopolymer guar gum solutions were studied systemically in terms of solubility, thickening performance, thermal and shear resistance, and proppant-carrying ability as well as gel-breaking performance in high-temperature and high-salt conditions. It is found that when investigated as a rheological modifier for fracturing fluids, both P3A and guar gum solutions exhibited good thickening performance and thermal and shear resistance. However, guar gum systems produced a large amount of solid residue after gel breaking, restricting their further development in oil recovery. In contrast, the P3A fracturing fluid systems had no residue but faced the problems of poor proppant suspension ability and high dosage. To solve these problems, P3A was directly crosslinked with organic zirconium in saturated brine to strengthen the fluid's microstructure. Rheological results indicate that crosslinked P3A solutions possess satisfying apparent viscosity compared with uncrosslinked ones. Furthermore, the temperature- and shear-resistant properties and proppant-carrying ability of such a fracturing fluid system exhibited a great improvement. These results suggest that the crosslinked synthetic polymer solutions exhibit a prominent rheological feature and hold promise application in high-temperature and high-salt reservoirs. In a word, this study provides not only a new material for hydrofracturing fluid development but also a novel direction for synthetic polymers to progress in the oil and gas industry in the future.

4. EXPERIMENTAL SECTION

4.1. Materials. P3A and guar gum were kindly supplied by Daqing Oilfield Company (China). The molar percentages of AM, acrylic acid (AA), and AMPS in P3A are 74.0, 23.7, and 2.3%, respectively, and its viscosity average molecular weight is 26.8×10^6 g·mol^{-1}.[25] NaCl (99.5%), NaOH (96.0%), ammonium persulfate (APS, 98.0%), zirconyl chloride (99.0%), glycerin (99.0%), and lactic acid (80.0%) were purchased from Chengdu Kelong Chemical Reagents Corporation (China) and were used without further purification. The silica sand (20−50 mesh) as a proppant was purchased from Shanghai Titan Scientific Co., Ltd. (China). Deionized water with a resistivity of 18.25 MΩ·cm^{-1} was prepared by using an ultrapure water purification system (CDUPT-III, Chengdu Ultrapure Technology Co., Ltd., China).

4.2. Preparation of the Hydrofracturing Fluid. A designed amount of P3A or guar gum was dissolved in solute to obtain the P3A or guar gum fracturing fluid system. The crosslinked P3A fracturing fluid was prepared as follows: a set amount of Zr crosslinker was added dropwise to P3A fracturing fluid while stirring to afford the final fluid.

4.3. Preparation of the Zr Crosslinker. A Zr crosslinker was prepared as follows: 10.0 g of zirconyl chloride, 6.0 g of glycerin, and 7.5 g of lactic acid were added to 10.0 g of ultrapure water and reacted at 75 °C for 3 h. Then, the pH value of the mixture was adjusted to 4.5 by adding 5.0 M NaOH solution.

4.4. Characterization. Scanning electron microscopy (SEM) measurements were carried out on a JSM-7500F field emission scanning electron microscope at an accelerating voltage of 20 kV. Infrared (IR) spectroscopy measurements were carried out with an EQUINX55 in the 500−4000 cm^{-1} range.

4.5. Rheology. All of the rheological tests were implemented by using a Physica MCR 302 (Anton Paar, Austria) rotational rheometer. The high-pressure and high-temperature cell DG35.12 system was employed at a high temperature (≥100 °C) under a designed pressure of ∼1.0 MPa. The Searle-type concentric cylinder geometry CC27 system was used at a relatively low temperature (<100 °C). In all of the experiments, the sample solutions were stabilized at the testing temperature for 5 min prior to data acquisition.

4.6. Evaluation of Hydrofracking Fluid Performances.

4.6.1. Dissolution Performance. In the dissolubility test, solid specimens were mixed with aqueous solution with different NaCl concentrations ranging from 0 to 5.0, 10.0, 15.0, 20.0, and 26.0 wt % and then continuously stirred at 25 °C. In the dissolution time test, solid specimens were mixed with saturated NaCl solution and then quickly dumped into a measuring cup of the CC27 system of the Physica MCR 302 rotational rheometer. The apparent viscosity was monitored at the fixed shear rate of 170 s^{-1} at 30 °C. The dissolution time was confirmed when the apparent viscosity reached a stable value.

4.6.2. Steady-State Rheological Performance. Sample solutions were dumped into a measuring cup of the CC27 system of the Physica MCR 302 rotational rheometer. The apparent viscosity was monitored at various shear rates ranging from 0.001 to 1000 s^{-1} at 25 °C.

4.6.3. Temperature and Shear Resistance. Sample solutions were conducted to a measuring cup of the DG35.12 system of the Physica MCR 302 rotational rheometer. The apparent viscosity was monitored at a fixed shear rate of 170 s^{-1}, and the temperature was first scanned from 20 to 100 °C with a heating rate of 3 °C·min^{-1}, followed by holding at 100 °C for 60 min.

4.6.4. Proppant-Carrying Capacity. Silica sands were mixed with sample solutions and stirred for 1 h at 25 °C. The ultimate volume fraction of proppants was 15%. The well-mixed samples were transferred to 50 mL graduated cylinders and were placed in an oven at 100 °C. Photos were taken every half an hour until particles completely settled down.

4.6.5. Gel-Breaking Performance. A certain amount of APS as a gel breaker was added to the homogeneous solution under stirring for 1 h in 25 °C for complete dissolution. The resulting solution was then transferred to a sealed container, which was placed in an oven at 100 °C. After predetermined heating times, the supernatant fluid was taken out for viscosity measurement with the CC27 system of the Physica MCR 302 rotational rheometer. The gel-breaking time was determined as the time required to reach a viscosity lower than 5 mPa·s. The residues were separated from broken fluids by using a centrifuge, washed with pure water to remove NaCl,

https://doi.org/10.1021/acsomega.1c03394
ACS Omega 2021, 6, 25421−25429

and then dried in an oven at 60 °C until constant weight was reached.

AUTHOR INFORMATION

Corresponding Author

Hongyao Yin − *Polymer Research Institute, State Key Laboratory of Polymer Materials Engineering, Sichuan University, Chengdu 610065, China;* orcid.org/0000-0002-0278-1862; Email: hyyin@scu.edu.cn

Authors

Xiaoqin Cao − *Polymer Research Institute, State Key Laboratory of Polymer Materials Engineering, Sichuan University, Chengdu 610065, China*

Yiwen Shi − *Sichuan University-Pittsburgh Institute, Sichuan University, Chengdu 610065, China*

Wenzhi Li − *Polymer Research Institute, State Key Laboratory of Polymer Materials Engineering, Sichuan University, Chengdu 610065, China*

Peiyun Zeng − *Polymer Research Institute, State Key Laboratory of Polymer Materials Engineering, Sichuan University, Chengdu 610065, China*

Zhuo Zheng − *Polymer Research Institute, State Key Laboratory of Polymer Materials Engineering, Sichuan University, Chengdu 610065, China*

Yujun Feng − *Polymer Research Institute, State Key Laboratory of Polymer Materials Engineering, Sichuan University, Chengdu 610065, China;* orcid.org/0000-0001-5046-6085

Complete contact information is available at: https://pubs.acs.org/10.1021/acsomega.1c03394

Author Contributions

The manuscript was written through contributions of all authors. All authors have given approval to the final version of the manuscript.

Notes

The authors declare no competing financial interest.

ACKNOWLEDGMENTS

This work is financially supported by the National Natural Science Foundation of China (grant no. U1762218), State Key Laboratory of Polymer Materials Engineering (grant no. SKLPME2020-3-10), and PetroChina Innovation Foundation (2019D-5007-0217).

REFERENCES

(1) Firozjaii, A. M.; Saghafi, H. R. Review on chemical enhanced oil recovery using polymer flooding: fundamentals, experimental and numerical simulation. *Petroleum* **2020**, *6*, 115−122.

(2) Liew, M. S.; Danyaro, K. U.; Zawawi, N. A. W. A. A comprehensive guide to different fracturing technologies: A review. *Energies* **2020**, *13*, 3326−3345.

(3) Barati, R.; Liang, J.-T. A review of fracturing fluid systems used for hydraulic fracturing of oil and gas wells. *J. Appl. Polym. Sci.* **2014**, *131*, 40735−40745.

(4) Saba, B. Potential treatment options for hydraulic fracturing return fluids: A review. *ChemBioEng Rev.* **2014**, *1*, 273−279.

(5) Al-Muntasheri, G. A. A critical review of hydraulic-fracturing fluids for moderate-to ultralow- permeability fromations over the last decade. *SPE Prod. Oper.* **2014**, *29*, 243−260.

(6) Al-Hameedi, A. T. T.; Alkinani, H. H.; Dunn-Norman, S.; Trevino, H. A.; Al-Alwani, M. A. *Conventional and eco-friendly hydraulic fracturing fluid additives: A review*; Paper presented at the SPE Hydraulic Fracturing Technology Conference and Exhibition: The Woodlands, Texas, USA, 1−18 Feb, 2020.

(7) Kreipl, M. P.; Kreipl, A. T. Hydraulic fracturing fluids and their environmental impact: then, today, and tomorrow. *Environ. Earth Sci.* **2017**, *76*, 160−175.

(8) Weaver, J.; Schmelzl, E.; Jamieson, M.; Schiffner, G. *New fluid technology allows fracturing without internal breakers*; SPE Gas Technology Symposium: Calgary, 2002.

(9) Shi, C. F.; Du, Q. L.; Zhu, L. H.; Zhang, S. Y.; Zhang, L.; Jian, X. W. Research on remaining oil distribution and further development methods for different kinds of oil layers in Daqing oilfield at high water-cut stage. Paper SPE 101034 presented at the *SPE Asia Pacific Oil and Gas Conference and Exhibition*; SPE: held in Adelaide, Australia, September 11−13, 2006.

(10) Jung, H. B.; Carroll, K. C.; Kabilan, S.; Heldebrant, D. J.; Hoyt, D.; Zhong, L.; Varga, T.; Stephens, S.; Adams, L.; Bonneville, A.; Kuprata, A.; Fernandez, C. A. Stimuli-responsive/rheoreversible hydraulic fracturing fluids as a greener alternative to support geothermal and fossil energy production. *Green Chem.* **2015**, *17*, 2799−2812.

(11) Zhao, G.; Dai, C.; Wang, S.; Zhao, M. Synthesis and application of nonionic polyacrylamide with controlled molecular weight for fracturing in low permeability oil reservoirs. *J. Appl. Polym. Sci.* **2014**, *132*, 41637.

(12) Li, X.; Xu, Z.; Yin, H.; Feng, Y.; Quan, H. Comparative studies on enhanced oil recovery: Thermoviscosifying polymer versus polyacrylamide. *Energ. Fuel.* **2017**, *31*, 2479−2487.

(13) Wever, D. A. Z.; Picchioni, F.; Broekhuis, A. A. Polymers for enhanced oil recovery: a paradigm for structure−property relationship in aqueous solution. *Prog. Polym. Sci.* **2011**, *36*, 1558−1628.

(14) Cai, S.; He, X.; Liu, K.; Zhang, R.; Chen, L. Interaction between HPAM and urea in aqueous solution and rheological properties. *Iran. Polym. J.* **2015**, *24*, 663−670.

(15) Samanta, A.; Ojha, K.; Sarkar, A.; Mandal, A. Mobility control and enhanced oil recovery using partially hydrolysed polyacrylamide (PHPA). *Int. J. Oil, Gas Coal Technol.* **2013**, *6*, 245−258.

(16) Samanta, A.; Bera, A.; Ojha, K.; Mandal, A. Effects of alkali, salts, and surfactant on rheological behavior of partially hydrolyzed polyacrylamide solutions. *J. Chem. Eng. Data* **2010**, *55*, 4315−4322.

(17) Doe, P. H.; Moradi-Araghi, A.; Shaw, J. E.; Stahl, G. A. Development and evaluation of EOR polymers suitable for hostile environments part 1: copolymers of vinylpyrrolidone and acrylamide. *SPE Reservoir Eng.* **1987**, *2*, 461−467.

(18) Liu, X. J.; Jiang, W. C.; Gou, S. H.; Ye, Z. B.; Xie, X. D. Synthesis and evaluation of a watersoluble acrylamide binary sulfonates copolymer on MMT crystalline interspace and EOR. *J. Appl. Polym. Sci.* **2012**, *125*, 1252−1260.

(19) Li, X.; Yin, H.-Y.; Zhang, R.-S.; Cui, J.; Wu, J.-W.; Feng, Y.-J. A salt-induced viscosifying smart polymer for fracturing inter-salt shale oil reservoirs. *Petrol. Sci.* **2019**, *16*, 816−829.

(20) Wang, Y.; Feng, Y.; Wang, B.; Lu, Z. A novel thermoviscosifying water-soluble polymer: synthesis and aqueous solution properties. *J. Appl. Polym. Sci.* **2010**, *116*, 3516−3524.

(21) Shah, A.; Fishwick, R.; Wood, J.; Leeke, G.; Rigby, S.; Greaves, M. A review of novel techniques for heavy oil and bitumen extraction and upgrading. *Energy Environ. Sci.* **2010**, *3*, 700−714.

(22) Kamal, M. S.; Sultan, A. S.; Al-Mubaiyedh, U. A.; Hussein, I. A.; Feng, Y. Rheological properties of thermoviscosifying polymers in high-temperature and high-salt environments. *Can. J. Chem. Eng.* **2015**, *93*, 1194−1200.

(23) Li, S.; Braun, O.; Lauber, L.; Leblanc, T.; Su, X.; Feng, Y. Enhancing oil recovery from high-temperature and high-salt reservoirs with smart thermoviscosifying polymers: a laboratory study. *Fuel* **2021**, *288*, 119777−119788.

(24) Ning, L. Current status and understanding of Jianghan shale gas development. In *The 2nd national special gas reservoir development technology seminar, Chongqing, China*; CNPC, 2013; 91−97.

(25) Zhang, Y.; Yin, H.; Feng, Y. Oppositely charged polyelectrolyte complexes for high-salt hydrofracking fluid. *Ind. Eng. Chem. Res.* **2019**, *58*, 18488−18497.
(26) Hurnaus, T.; Plank, J. Crosslinking of guar gum and HPG based fracturing fluids using ZrO_2 nanoparticles. In *SPE-173778-MS Paper Presented at the SPE Interational Symposium on Oilfield Chemistry*; SPE: The Woodlands, Texas, USA, 1−15 Apr, 2015.
(27) Zhao, J. Z.; Jia, H.; Pu, W. F.; Liao, R. Influences of fracture aperture on the water-shutoff performance of polyethyleneimine cross-linking partially hydrolyzed polyacrylamide gels in hydraulic fractured reservoirs. *Energy Fuels* **2011**, *25*, 2616−2624.
(28) Bao, Y.; Ma, J.; Li, N. Synthesis and swelling behaviors of sodium carboxymethyl cellulose-g-poly(AA-co-AM-co-AMPS)/MMT superabsorbent hydrogel. *Carbohydr. Polym.* **2011**, *84*, 76−82.
(29) Zhao, Q.; Zhao, L.; Ma, C. Synthesis and properties of fluorinated hydrophobic association polyacrylamide as thickener for hydraulic fracturing fluid. *Iran. Polym. J.* **2017**, *26*, 589−595.
(30) Zhao, G.; Dai, C.; You, Q.; Zhao, M.; Zhao, J. Study on fromation of gels formed by polymer and zirconium acetate. *J. Sol.-Gel. Sci. Technol.* **2013**, *65*, 392−398.
(31) Rose, J.; De Bruin, T. J. M.; Chauveteau, G.; Tabary, R.; Hazemann, J.-L.; Proux, O.; Omari, A.; Toulhoat, H.; Bottero, J.-Y. Aqueous zirconium complexes for gelling polymers. A combined X-ray absorption spectroscopy and quantum mechanical study. *J. Phys. Chem. B* **2003**, *107*, 2910−2920.
(32) Intorre, B. I.; Martell, A. E. Zirconium complexes in aqueous solution. I. reaction with multidentate ligands. *J. Am. Chem. Soc.* **1960**, *82*, 358−364.
(33) Clearfield, A. The mechanism of hydrolytic polymerization of zirconyl solutions. *J. Mater. Res.* **1990**, *5*, 161−162.
(34) Omari, A. Gelation control of the scleroglucan-zirconium system using oxyacids. *Polymer* **1995**, *36*, 4263−4265.

https://doi.org/10.1021/acsomega.1c03394
ACS Omega 2021, 6, 25421−25429